

# Doniach Diagram of Disordered Electron Systems

Hyun Yong Lee<sup>1</sup> and Stefan Kettemann<sup>1,2</sup>

<sup>1</sup>*Division of Advanced Materials Science, Pohang University of Science and Technology (POSTECH), Pohang 790-784, South Korea\**

<sup>2</sup>*School of Engineering and Science, Jacobs University Bremen, Bremen 28759, Germany<sup>†</sup>*  
(Dated: February 20, 2019)

We have derived the quantum phase diagram of disordered electron systems as function of the concentration of magnetic impurities  $n_m$  and the local exchange coupling  $J$ . The competition between RKKY interaction  $J_{\text{RKKY}}$  and the Kondo effect gives rise to a rich magnetic quantum phase diagram, the Doniach diagram. Our numerical results show that both the Kondo temperature  $T_K$  and  $J_{\text{RKKY}}$  are widely distributed and the quantum critical point is extended to a critical region. We find a sharp cutoff in the wide distribution of their ratio,  $J_{\text{RKKY}}/T_K$ , which allows us to define a critical density of magnetic impurities  $n_c$  below which Kondo screening wins at all sites of the system above a critical coupling  $J_c$ . We find that a spin coupled phase grows at the expense of the Kondo phase as disorder is increased. We derive the magnetic susceptibility, showing anomalous power law behavior. In the Kondo regime that power is determined by the wide distribution of the Kondo temperature, while in the spin coupled phase it is governed by the distribution of  $J_{\text{RKKY}}$ . At low densities and small  $J < J_c$  we identify a paramagnetic phase. At high concentrations  $n_m$  there is a transition to a spin glass phase followed by a magnetic phase with long range order.

Phenomena which emerge from the interplay of strong correlations and disorder remain a challenge for condensed matter theory. Spin correlations and disorder effects are however relevant for a wide range of materials, including doped semiconductors like Si:P close to metal-insulator transitions[1], and heavy Fermion systems, materials with 4f or 5f atoms, notably Ce, Yb, or U[2, 3]. Many of these materials show a remarkable magnetic quantum phase transition which can be understood by the competition between indirect exchange interaction, the Ruderman-Kittel-Kasuya-Yoshida (RKKY) interaction between localised magnetic moments[4–6] and their Kondo screening. Thereby, one finds a suppression of long range magnetic order when exchange coupling  $J$  is increased and Kondo screening succeeds. This results in a typical quantum phase diagram with a quantum critical point where the  $T_c$  of the magnetic phase is vanishing, the Doniach diagram[7]. Recently, controlled studies of magnetic adatoms on the surface of metals[8], on graphene[9], and on the conducting surface of topological insulators[10] with surface sensitive experimental methods like spin resolved STM and ARPES became possible. This demands a theoretical study of the Doniach diagram for magnetically doped disordered electron systems (DES), in particular 2D systems.

In any material there is some degree of disorder. In doped semiconductors it arises from the random positioning of the dopants themselves, in heavy Fermion metals and in 2D metals it may arise from structural defects or impurities. Disorder is known to cause Anderson localisation, which therefore has to be taken into account when deriving the Doniach diagram of disordered electron systems. Moreover, as noted already early[11], the physics of random systems is fully described by probability distributions, not just averages. This must be

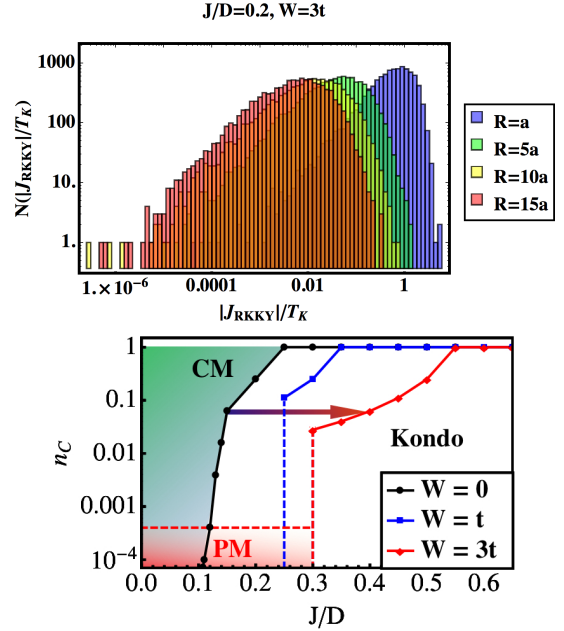


FIG. 1. (Color online) Top: Distribution of the ratio between  $|J_{\text{RKKY}}|$  and  $T_K$  for various distances  $R$ . Bottom: Critical MI density  $n_c$  as function of  $J/D$  for various disorder strengths  $W$  as determined by the distance  $R$  below which  $|J_{\text{RKKY}}|/T_K$  does not exceed 1 at any site. Horizontal dashed line: density  $n_\xi$  below which there is a paramagnetic moment phase (PM). CM= phase with coupled magnetic moments.

particularly true for systems with random local magnetic impurities (MIs)[12], since the magnetic impurities are exposed to the local density of states of the conduction electrons, which is widely distributed itself. In fact, it has been noticed that a wide distribution of the Kondo temperature  $T_K$  of MIs in disordered host metals gives rise to non-Fermi liquid behavior, such as the

low temperature power-law divergence of the magnetic susceptibility [3, 12–19]. Nonmagnetic disorder quenches the Kondo screening of MIs due to Anderson-localisation and the formation of local pseudogaps at the Fermi energy [18, 20–22], resulting in bimodal distributions of  $T_K$  and a finite concentration of free, paramagnetic moments (PMs). However, in these studies the RKKY interaction  $J_{\text{RKKY}}$  between different MIs has not yet been taken into account.  $J_{\text{RKKY}}$  is mediated by the conduction electrons, and aligns the spins of the MIs ferromagnetically or antiferromagnetically, depending on their distance  $R$ . This is a long-ranged interaction, with a power law decay  $J_{\text{RKKY}} \sim 1/R^d$ , where  $d$  is the dimension, and its typical value is not changed by weak disorder[23–26]. However, its amplitude has a wide log-normal distribution in disordered metals[23, 27]. Thus, in order to obtain the Doniach diagram of random  $T_K$  and  $J_{\text{RKKY}}$ , we start from a microscopic description of the MIs, the Anderson impurity model coupled to a non-interacting disordered electronic Hamiltonian with on-site disorder. Then we map it with the Schrieffer-Wolff transformation on a model of Kondo impurity spins coupled to the disordered host electron spins by the local coupling  $J$  [22]. For the numerical calculations we employ the single-band Anderson tight-binding model on a square lattice of size  $L$  and lattice spacing  $a$ ,  $H = -t \sum_{\langle i,j \rangle} c_i^\dagger c_j + \sum_i (w_i - \tilde{E}_F) c_i^\dagger c_i$ , where  $t$  is the hopping energy between nearest neighbours  $\langle i, j \rangle$ ,  $w_i$  is the on-site disorder potential distributed in the interval  $[-W/2, W/2]$ .  $\tilde{E}_F = E_F + \varepsilon_{\text{edge}}$ , where  $E_F$  is the Fermi energy measured from the band edge, in 2D  $\varepsilon_{\text{edge}} = -4t$ . We use periodic boundary conditions.

We obtain  $T_K$  at position  $\mathbf{R}_i$  from[28]

$$1 = \frac{J}{2} \int_0^D d\varepsilon \frac{\tanh[(\varepsilon - E_F)/2T_K]}{\varepsilon - E_F} \rho_{ii}(\varepsilon), \quad (1)$$

with band width  $D$ .  $\rho_{ii}(\varepsilon) = \langle i | \delta(\varepsilon - H) | i \rangle$  is the local density of states (LDOS). The RKKY coupling  $J_{\text{RKKY}}_{ij}$  between two MIs located at positions  $\mathbf{R}_i, \mathbf{R}_j$  is in the zero temperature limit ( $T = 0$ ) given by[26, 29]

$$J_{\text{RKKY}}_{ij} = -J^2 \frac{S(S+1)}{2S^2} \int_{\varepsilon < E_F} d\varepsilon \int_{\varepsilon' > E_F} d\varepsilon' \frac{F(\varepsilon, \varepsilon')_{ij}}{\varepsilon - \varepsilon'}, \quad (2)$$

where  $F(\varepsilon, \varepsilon')_{ij} = \text{Re}[\rho_{ij}(\varepsilon)\rho_{ji}(\varepsilon')]$ , and  $S$  is the magnitude of the MI spin. Using the Kernel Polynomial method (KPM) [29, 30], one can evaluate the matrix elements of the local density of states  $\rho_{ij}(\varepsilon) = \langle i | \delta(\varepsilon - \hat{H}) | j \rangle$ [26, 30, 31] with a Polynomial expansion of order  $M$ . In order to ensure convergence, but avoid finite size effects, we increased  $M$  linearly with  $L$ [27], for an explanation see Ref.32. Eq.(2) yields in a clean 2D system  $J_{\text{2D}}^0 = -\frac{m^*}{8\pi} \sin(2k_F R)/(k_F R)^2$  in the asymptotic limit  $k_F R \gg 1$  with effective electron mass  $m^* = 1/(2a^2t)$ , and Fermi wave vector  $k_F$  [4]. Its geometrical average is close to the clean limit for distances  $R$

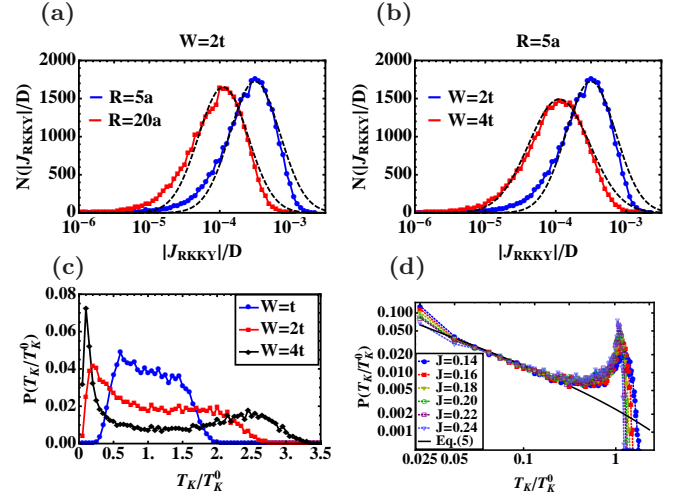


FIG. 2. (Color online)  $N(|J_{\text{RKKY}}|)$  at (a) fixed disorder strength  $W = 2t$ , (b) fixed  $R = 5a$  ( $N = 30\,000$ ,  $L = 100a$ ,  $M = 1000$ ). Black dashed lines: fit to log-normal distribution. (c)  $P(T_K)$  at fixed  $j = J/D = 0.25$ , (d)  $P(T_K)$  at fixed  $W = 5t$  ( $N=30\,000$ ,  $L=40a$ ,  $M=200$ ).  $E_F = 2t$  in a)-d).

smaller than localisation length  $\xi$ , and decays exponentially at larger distances[26, 33],  $e^{\langle \frac{1}{2} \ln J_{\text{RKKY}}^2 \rangle} \sim e^{-R/\xi}$ . However, as shown in Figs.2 a, b, the absolute value of  $J_{\text{RKKY}}$  is widely distributed and well fitted by a log-normal distribution,  $P(x) = \frac{N}{\sqrt{2\pi\sigma}} \exp\left[-\frac{(x-x_0)^2}{2\sigma^2}\right]$ , where  $x = \ln|J_{\text{RKKY}}|$  and the fitting gives for  $R = 5a$  and  $W = 2t, 4t$ ,  $x_0 = 5, 6$  and width  $\sigma = 5.3 + .85W/t$  increasing with the disorder strength  $W$ , consistent with analytical results obtained at weak disorder[23], while it hardly depends on the distance  $R$ . We used  $N = 30\,000$  disorder configurations.

The distribution of  $T_K$  is shown in Fig.2 c, as obtained from the numerical solution of Eq. (1) for  $L = 40a$ ,  $j = J/D = 0.25$ . Since for every sample only one single site is taken to avoid a distortion of the distribution due to intersite correlations, we had to use a huge number of  $N = 30\,000$  different random disorder configurations to get sufficient statistics. It has a strongly bimodal shape where the low  $T_K$ -peak becomes more distinctive with larger disorder amplitude  $W$ [17, 18, 34]. In Fig.2 d we show these results for fixed disorder strength  $W = 5t$  for various exchange couplings  $j$ . Recently, an analytical derivation of the low  $T_K$ -tail of  $P(T_K)$  was done, using the multifractal distribution and correlations of intensities[22]. These correlations are in 2D logarithmic with an amplitude of order  $1/g$ , where  $g = E_F\tau$ . For weak disorder,  $g \gg 1$ , it corresponds to a power law correlation with power  $\eta_{2D} = 2/\pi g$ . The correlation energy is of the order of the elastic scattering rate  $E_c \sim 1/\tau$ . Thus, for  $T_K \ll \text{Max}\{\Delta_\xi = D/\xi^2, \Delta = D/L^2\}$ [22],

$$P(T_K) = (1 - p_{FM}) \left(\frac{E_c}{T_K}\right)^{1-j} (\text{Min}\{\xi, L\})^{-\frac{d^2 j^2}{2\eta_{2D}}}, \quad (3)$$

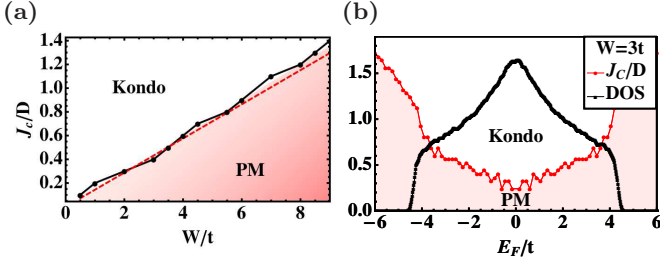


FIG. 3. (Color online) Quantum phase diagram with paramagnetic moment phase (PM) and Kondo screened phase: Critical exchange coupling  $J_c/D$  ( $L = 100$ ) (a) as function of  $W$  ( $M = 300, E_F = 2t$ ). Red dashed line: Eq. (5). (b) as function of Fermi energy  $E_F$  ( $M = 200$ ); Red line: (DOS).

where  $p_{FM} = n_{FM}(0)/n = (\text{Min}\{\xi, L\})^{-\frac{d^2 j^2}{2\eta_{2D}}}$ , the ratio of free PMs. Eq. (3) has a power law tail with power  $\beta_j = 1 - j$  in good agreement with the numerical results, Fig. 2 d, for  $T_K/T_K^0 < .03$ . For  $T_K^0 > T_K > \text{Max}\{\Delta_\xi = D/\xi^2, \Delta = D/L^2\}$  one finds [22]

$$\frac{P(T_K)}{1 - p_{FM}} = \left(\frac{E_c}{T_K}\right)^{1 - \frac{\eta_{2D}}{2d}} \exp\left[-\frac{\left(\frac{T_K}{E_c}\right)^{\frac{\eta_{2D}}{d}}}{2c_1} \ln^2\left(\frac{T_K}{T_K^0}\right)\right], \quad (4)$$

where  $c_1 = 7.51$ . This expression is in agreement with the numerical results, see Fig. 2 d, using  $\xi = g \exp(\pi g)$ , and  $1/\tau = \pi W^2/6D$ , fitting only  $E_c \approx .73t$  and the prefactor. Thus, we confirm that the power law tail is governed by the multifractal correlation with power  $\eta_{2D}$ .

The quantum phase transition between the free paramagnetic moment phase (PM) and a Kondo screened phase can be studied by calculating the critical exchange coupling  $J_c$  above which there is no more than one free magnetic moment in the sample volume  $L^d$  [20]. From the multifractality of the eigenfunction intensities it is found to be related to the power  $\eta_{2D}$  of the power law correlations in the 2D DES as  $J_c = \sqrt{\eta_{2D} D}$  and thus to increase in 2D linearly with disorder strength  $W$  as [22],

$$J_c = \sqrt{D/(3E_F)W}. \quad (5)$$

In Fig. 3 a, Eq. (5) is plotted together with numerical results as function of disorder strength  $W$ . We find good agreement. There are only deviations at large disorder,  $g < 1$ , where the  $1/g$  expansion breaks down. We plot  $J_c$  as function of  $E_F$  in Fig. 3 b, together with the density of states (DOS). We find that  $J_c$  is increasing towards the band edge as  $1/\sqrt{E_F}$  in agreement with Eq. (5). Far outside of  $\varepsilon_{\text{edge}}$  of the clean system it increases as  $J_c/D = 1/\ln|\varepsilon_{\text{edge}} - E_F|$  due to the gap in the DOS.

*Doniach Phase Diagram.* In clean systems the critical density  $n_c = 1/R_c^d$  above which the MIs are coupled with each other is obtained from the condition that  $|J_{\text{RKKY}}^0(R_c)| = T_K$  [7]. This yields in 2D with  $|J_{\text{RKKY}}^0|_{k_F R \gg 1} = J^2 \frac{m}{8\pi^2 k_F^2 R^2}$  and  $T_K = cE_F \exp(-D/J)$ ,  $c \approx 1.14$ ,  $n_c = 16\pi^2 c \frac{E_F}{J^2} \exp(-\frac{D}{J})$ .

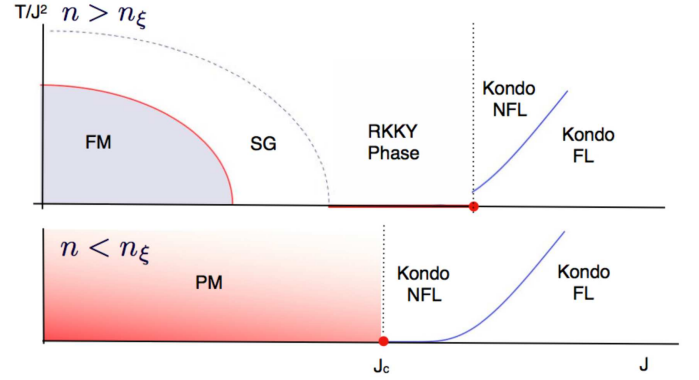


FIG. 4. (Color online) Doniach diagram: temperature  $T$  divided by  $J^2$  versus  $J/D$ . Vertical dotted line: critical point  $J_c(n)$  separating RKKY phase from Kondo phase. Blue line:  $T^*(n)$  separating Kondo FL phase from Kondo NFL phase. For  $n < n_\xi$  and  $J < J_c$  a paramagnetic phase (PM) appears.

In disordered systems,  $T_K$  at a certain site competes with the RKKY coupling to another MI at distance  $R$ . Thus, the distribution function of the ratio of these two energy scales  $x_{JK} = |J_{\text{RKKY}}(R)|/T_K$  is needed for a given disordered sample with density of MIs  $n = 1/R^2$ , where  $R$  is the average distance between the MIs. The distribution of  $x_{JK}$  for  $W = 3t$  and  $J/D = 0.2$  is shown for several  $R$  in Fig. 1 (top) ( $N = 10000$ ,  $L = 100a$ ,  $E_F = t$  and  $M = 300$ ). We see that the distribution has a sharp upper cutoff in  $x_{JK}$ , allowing us to define a critical density  $n_c(J) = 1/R_c^2$  below which the Kondo effect dominates in the competition with RKKY interaction at all sites.  $n_c(J)$  is plotted in Fig. 1 (bottom) for various values of disorder strength  $W$ . When the MI density  $n$  exceeds  $n_c$ , magnetic clusters start to form at some sites and the MIs may be coupled by  $J_{\text{RKKY}}$ . We see that this coupled moment phase (CM) expands at the expense of the Kondo phase with increasing  $W$ . When  $R$  is larger than localisation length  $\xi$  the coupling  $J_{\text{RKKY}}$  is exponentially small and there is a *paramagnetic phase* (PM) below  $n_\xi = 1/\xi(g)^2$ , where MIs remain free up to exponentially small temperatures.

We find, that the Kondo phase splits at finite temperature into a *Kondo Fermi-liquid (FL) phase*, where all MIs are screened, and a *Kondo Non-Fermi-liquid (NFL) phase* where some MIs remain unscreened and contribute to the magnetic susceptibility with an anomalous temperature dependence, given by [22],

$$\chi(T) \sim \frac{n}{E_c} \frac{2d}{\eta_{2D}} \left(\frac{T}{E_c}\right)^{\frac{\eta_{2D}}{2d} - 1} \text{ for } T > \frac{D}{\xi^2}. \quad (6)$$

The temperature  $T^*(n)$ , see Fig. 4 (blue line), is given by the position of the low  $T_K$  peak in  $P(T_K)$ , see Fig. 2 c. We note that  $J$  may be distributed itself and may add a nonuniversal, material dependent contribution to the distribution of  $T_K$  [15] and  $J_{\text{RKKY}}$ .

For  $n > n_c$  there is a succession of phases, the *RKKY phase* where clusters are formed locally due to the widely distributed RKKY coupling. Anomalous power laws are observed when clusters are broken up successively as temperature is raised. From the log-normal distribution  $N(|J_{RKKY}|)$  one obtains for the magnetic susceptibility,  $\chi(T)T = n_{FM}(T) = \int_0^T d|J_{RKKY}|N(|J_{RKKY}|) \sim n \exp[-\ln^2(T/|J_{RKKY}^0|)/(2\sigma(W))^2]$ , where width  $\sigma(W)$  increases with disorder strength  $W$ . Accordingly, the excess specific heat is  $C(T) = T \frac{dn_{FM}}{dT} \sim \exp[-\ln^2(T/|J_{RKKY}^0|)/(2\sigma(W))^2]$ . At higher concentrations  $n > n_{SG}$  a *spin-glass phase* appears, where the magnetic susceptibility shows a peak at spin glass temperature  $T_{SG}$  as studied in Refs.[35, 36]. Above a critical density  $n_F$  a phase with long range order may form below a critical temperature  $T_c(n, J)$ [36–39].

*Conclusions.* While the ratio of RKKY coupling and Kondo temperature  $|J_{RKKY}|/T_K$  is found to be widely distributed, we find a sharp cutoff of its distribution function which allows us to define a critical density of magnetic impurities  $n_c$  below which Kondo wins at all positions in a disordered sample above a critical coupling  $J_c$ . As a result, a phase where the MI spins are coupled grows at the expense of the Kondo phase as disorder is increased. The magnetic susceptibility obeys an anomalous power law behavior, which crosses over from the Kondo regime where that power is determined by the wide distribution of the Kondo temperature, while in the spin coupled phase it is governed by the log-normal distribution of  $J_{RKKY}$ . At low densities and small  $J < J_c$  we identify a paramagnetic phase. The distribution function of  $|J_{RKKY}|/T_K$  is expected to determine also the magnetic phase diagram of magnetically doped graphene, the surface of topological insulators with magnetic adatoms[40]. It may also explain the anomalous magnetic properties of doped semiconductors in the vicinity of metal-insulator transition[1], where we expect that  $\eta$  is replaced by the universal value  $\eta = 2(\alpha_0 - d)$ ,  $d = 3$  with the universal multifractality parameter  $\alpha_0$ .

We gratefully acknowledge useful discussions with Georges Bouzerar, Ki-Seok Kim, Eduardo Mucciolo and Keith Slevin, as well as support by WCU through KOSEF (R31-2008-000-10059-0) in the Division of Advanced Materials Science.

---

\* hyunyongrhee@postech.edu

† s.kettemann@jacobs-university.de

- [1] H. v. Löhneysen, Adv. in Solid State Phys **40**, 143 (2000).  
 [2] H. v. Löhneysen, A. Rosch, M. Vojta, and P. Wölfle, Rev. Mod. Phys. **79**, 1015 (2007).  
 [3] E. Miranda and V. Dobrosavljevic, Reports on Progress in Physics **68**, 2337 (2005).  
 [4] M. A. Ruderman and C. Kittel, Phys. Rev. **96**, 99 (1954).

- [5] T. Kasuya, Progress of Theoretical Physics **16**, 45 (1956).  
 [6] K. Yosida, Phys. Rev. **106**, 893 (1957).  
 [7] S. Doniach, Physica B+C **91**, 231 (1977), ISSN 0378-4363.  
 [8] L. Zhou, J. Wiebe, S. Lounis, E. Vedmedenko, F. Meier, S. Blugel, P. H. Dederichs, and R. Wiesendanger, Nat. Phys. **6**, 187 (2010).  
 [9] J.-H. Chen, L. Li, W. G. Cullen, E. D. Williams, and M. S. Fuhrer, Nat. Phys. **7**, 1745 (2007).  
 [10] D. Hsieh, Y. Xia, L. Wray, D. Qian, A. Pal, J. H. Dil, J. Osterwalder, F. Meier, G. Bihlmayer, C. L. Kane, et al., Science **323**, 919 (2009).  
 [11] P. W. Anderson, Nobel Lectures in Physics **1980**, 376 (1977).  
 [12] Mott, N. F., J. Phys. Colloques **37**, C4 (1976).  
 [13] E. Miranda, V. Dobrosavljevic, and G. Kotliar, Journal of Physics: Condensed Matter **8**, 9871 (1996).  
 [14] R. N. Bhatt and D. S. Fisher, Phys. Rev. Lett. **68**, 3072 (1992).  
 [15] A. Langenfeld and P. Wlfle, Annalen der Physik **507**, 43 (1995), ISSN 1521-3889.  
 [16] A. Castro Neto and B. Jones, Phys. Rev. B **62**, 14975 (2000).  
 [17] P. S. Cornaglia, D. R. Grempel, and C. A. Balseiro, Phys. Rev. Lett. **96**, 117209 (2006).  
 [18] S. Kettemann and E. R. Mucciolo, Phys. Rev. B **75**, 184407 (2007).  
 [19] M.-T. Tran and K.-S. Kim, Phys. Rev. Lett. **105**, 116403 (2010).  
 [20] A. Zhuravlev, I. Zharekeshev, E. Gorelov, A. I. Lichtenstein, E. R. Mucciolo, and S. Kettemann, Phys. Rev. Lett. **99**, 247202 (2007).  
 [21] S. Kettemann and M. E. Raikh, Phys. Rev. Lett. **90**, 146601 (2003).  
 [22] S. Kettemann, E. R. Mucciolo, I. Varga, and K. Slevin, Phys. Rev. B **85**, 115112 (2012).  
 [23] I. V. Lerner, Phys. Rev. B **48**, 9462 (1993).  
 [24] L. N. Bulaevskii and S. V. Panyukov, JETP Lett. **43**, 240 (1986).  
 [25] G. Bergmann, Phys. Rev. B **36**, 2469 (1987).  
 [26] H. Lee, J. Kim, E. R. Mucciolo, G. Bouzerar, and S. Kettemann, Phys. Rev. B **85**, 075420 (2012).  
 [27] H. Lee, E. R. Mucciolo, G. Bouzerar, and S. Kettemann, Phys. Rev. B **86**, 205427 (2012).  
 [28] Y. Nagaoka, Phys. Rev. **138**, A1112 (1965).  
 [29] S. Roche and D. Mayou, Phys. Rev. B **60**, 322 (1999).  
 [30] A. Weiße, G. Wellein, A. Alvermann, and H. Fehske, Rev. Mod. Phys. **78**, 275 (2006).  
 [31] E. R. Mucciolo, unpublished (2010).  
 [32] P. Wenk and G. Bouzerar, unpublished (2012).  
 [33] J. A. Sobota, D. Tanasković, and V. Dobrosavljević, Phys. Rev. B **76**, 245106 (2007).  
 [34] S. Kettemann and E. Mucciolo, JETP Letters **83**, 240 (2006), ISSN 0021-3640.  
 [35] K. Binder and A. P. Young, Rev. Mod. Phys. **58**, 801 (1986).  
 [36] B. Coqblin, C. Lacroix, M. A. Gusmão, and J. R. Iglesias, Phys. Rev. B **67**, 064417 (2003).  
 [37] C. M. Varma, Rev. Mod. Phys. **48**, 219 (1976).  
 [38] S. G. Magalhaes, F. M. Zimmer, P. R. Krebs, and B. Coqblin, Phys. Rev. B **74**, 014427 (2006).  
 [39] G. Bouzerar, T. Ziman, and J. Kudrnovsky, Eur. Phys. Lett. **69**, 812 (2005).  
 [40] H. Lee and S. Kettemann, unpublished (2012).